Catalysis Today 176 (2011) 97–102

Contents lists available at ScienceDirect

Catalysis Today

journal homepage: www.elsevier.com/locate/cattod

Ethanol conversion in the presence of cobalt nanostructured oxides

Wojciech Gac*, Witold Zawadzki, Bogna Tomaszewska

Department of Chemical Technology, Faculty of Chemistry, University of Maria Curie-Sklodowska, 3M, Curie-Sklodowskia Sq., 20-031 Lublin, Poland

ARTICLE INFO

Article history:
Received 30 September 2010
Received in revised form
29 December 2010
Accepted 4 February 2011
Available online 8 March 2011

Keywords:
Cobalt catalyst
Nanocasting
Hydrogen
Steam reforming
Ethanol

ABSTRACT

The surface, structural, redox and catalytic properties of the catalysts obtained by the nanocasting technique with the use of silica mesoporous template were investigated. Ethanol conversion approached 100% at 420 °C for supported and 66% for unsupported cobalt catalysts, respectively. Complete conversion of ethanol was recorded at 480 °C for both catalysts. In such conditions, the unsupported system showed high hydrogen yield and low selectivity to CH_3CHO, CO and CH_4.

© 2011 Elsevier B.V. All rights reserved.

1. Introduction

Recently one can observe growing interests in the production and utilisation of hydrogen, especially in the field of the fuel cells. Alcohols are important group of compounds which can be obtained from the renewable sources. Hydrogen can be produced from alcohols in the dehydrogenation, partial oxidation or steam reforming reactions. The most active and selective catalysts in the steam reforming of methanol to carbon dioxide and hydrogen are copper-based, mainly Cu–ZnO–Al_2O_3 type catalysts and Pd catalysts modified with zinc oxide [1]. In the case of the steam reforming of ethanol, various groups of catalysts have been tested and described in the literature. High activity has been presented for noble metal catalysts, such as Pt, Rh, Pd, Ru [2–4], and transition metal, mainly nickel [4–7] and cobalt catalysts [8–16]. Numerous promoters, modifiers and supports, including Al_2O_3, MgO, SiO_2, CeO_2, ZrO_2, La_2O_3, Y_2O_3, CeO_2–ZrO_2, $SrTiO_3$, $MgAl_2O_4$ were examined. Wide application of the steam reforming of ethanol for the production of hydrogen is still limited, primarily due to insufficient coking resistance of the catalysts, their low selectivity to hydrogen, pronounced selectivity to carbon monoxide, acetone, acetaldehyde or methane. Though supports are used in catalysts mainly for achieving high dispersion and stabilization of metal crystallites, the active sites on the support surface participate in the reaction, enabling sorption of water and ethanol molecules. On the other hand, the support may also influence selectivity and promote coking, e.g. via transformation of ethanol to ethylene. Surface ethoxy species can be converted into various compounds, lacking the catalysts selectivity. Thus it was interesting to find if it is possible to use unsupported cobalt oxides, and to study properties of such systems. The catalytic properties of Co_3O_4 have been scarcely investigated in the reaction of steam reforming of ethanol. Beneficial properties of cobalt oxides obtained by the precipitation–oxidation method were presented by Wang [15]. In turn, Tuti stated, that the activity of reduced cobalt oxides prepared by thermal decomposition of cobalt nitrate at 750 °C was as good MgO supported systems [16].

Recently nanocasting technique has been used for the preparation of the series of interesting oxide materials [17–21]. In the first preparation stage of this technique, pores of matrices (e.g. of novel mesoporous silicas, alumina, carbons or polymers) are filled with the solution containing metal ions. After heat treatment, the matrices are removed by dissolution or combustion. The obtained materials may consist of agglomerates containing the species, formerly located in the pores. In some cases the oxide species may also attain structural features of pore system. The physical, optical and chemical properties of such systems are related to the preparation conditions and properties of templates used. Several research papers demonstrated the potential use of silica mesoporous materials of well ordered and uniform pores as matrices for the preparation of carbons, carbon nitride and metal oxides.

The aim of the studies was comparison of the surface, structural, redox and catalytic properties of cobalt catalysts prior and after silica mesoporous template removal in the ethanol steam reforming

* Corresponding author. Tel.: +48 815 375 526; fax: +48 815 375 565.
E-mail address: Wojciech.Gac@umcs.lublin.pl (W. Gac).

0920-5861/$ – see front matter © 2011 Elsevier B.V. All rights reserved.
doi:10.1016/j.cattod.2011.02.004

reaction. Such studies are crucial to make progress in the development of new multicomponent oxide catalysts.

2. Experimental

The MCM-48 type mesoporous silica was prepared according to the Ref. [22]. The obtained material was impregnated several times with 0.8 M ethanol solution of cobalt nitrate to obtain around 40 wt% of Co. The support was immersed in the solution for the 20 min and stirred in the ultrasonic conditions. The samples after each impregnation were dried at elevated temperatures, and finally calcined for 6 h at 500 °C. Part of this material was denoted as "Co–Si" catalyst. From the other part, silica was removed by the dissolution in 1 M NaOH solution. The oxides ware separated by centrifugation, washed with water, dried and then calcined at 500 °C (the resulted sample was marked as "Co").

Nitrogen adsorption/desorption isotherms at −196 °C were determined volumetrically using ASAP 2405 N analyzer (Micromeritics Corp., Norcross, GA). The BET specific surface area, S_{BET}, and the total pore volumes, V_t, were determined by applying the standard methods [23]. The calculations of pore size distributions followed the Barrett, Joyner and Halenda (BJH) procedure. X-ray powder diffraction (XRD) measurements were conducted with the upgraded Zeiss HZG-4 diffractometer using CuK_α radiation. X-ray photoelectron spectroscopy studies were performed in the UHV multichamber system (Prevac).

Redox properties of the samples were investigated by the temperature-programmed reduction method. The studies were carried out in the TPR apparatus AMI-1 (Zeton Altamira). The reduction process was conducted in the mixture of 6% H_2/Ar (Q = 30 ml/min) (Praxair). The rate of temperature increase was 10 °C/min. The evolved water was removed in a cold trap placed between the reactor and thermal conductivity detector (TCD).

Temperature programmed desorption of hydrogen was performed in the AMI-1 system. Samples (0.05 g) were reduced in a flow of hydrogen with the rate 20 °C/min up to 400 °C. Then, after 1 h they were cooled down. The desorption of hydrogen was performed after flushing the samples with argon (30 ml/min) for 20 min. The rate of temperature increase was 20 °C/min. A cold trap was placed between the reactor and thermal conductivity detector (TCD).

The steam reforming of ethanol was carried out under atmospheric pressure in a fixed bed continuous-flow quartz reactor, in the same conditions as described in Ref. [13]. The samples (0.1 g) were reduced in situ with hydrogen at 400 °C for 1 h, prior to the reaction. The catalysts were diluted (at the weight ratio of 1/10) with 0.15–0.3 mm grains of quartz in order to obtain the constant temperature in the catalytic layer. The aqueous solution of ethanol (10.85 wt%, the EtOH/water molar ratio equals 1/21) was supplied by a mass flow controller (Bronkhorst) to an evaporator (150 °C) and the reactant vapours, without diluting with any inert gas, were fed to the reactor at a flow rate of 0.268 mol/h. The temperature was increased step-by-step and the analyses of the reaction products were carried out several times for about 2 h of the reaction at each temperature. The analysis (all in gas phase) was carried out on-line by means of two gas chromatographs, Varian CP-3800 and Chromatron GCHF 18.3, respectively. The first one was equipped with two capillary columns, contained a porous polymer Poropak Q (for all organics, carbon dioxide and water vapour) and an activated molecular sieve 5A (for methane and carbon monoxide analysis). Helium was used as a carrier gas and a TCD detector was employed. The second chromatograph with an activated charcoal packed column, nitrogen as a carrier gas and a TCD detector was used for determination of hydrogen concentration. The sensitivity of the detectors to the analysed compounds (response factors) was determined, before and after each catalytic test, by their calibration against external standards of single compounds or their certified (Praxair) mixtures composed of carbon oxides and hydrocarbons in helium. The concentrations of the external standards were comparable with those of analysed products. The reproducibility of the analysis of the components of the certified mixtures was about ±2%. Because of some tailing of chromatographic peaks of water, the reproducibility of its analysis was lower than that of other compounds, about ±5 relative %.

The total conversion of ethanol X_{EtOH}, conversion of water X_{H_2O} and conversions of ethanol into particular carbon-containing products, X_{CP}, were calculated on the basis of their concentrations before and after the reaction, with a correction introduced for the volume change during the reaction, from the equations:

$$X_{CP} = \frac{c_{CP}^{out} \bullet K}{n/2 \bullet c_{EtOH}^{in}} \times 100(\%), \quad X_{EtOH} = \frac{c_{EtOH}^{in} - c_{EtOH}^{out} \bullet K}{c_{EtOH}^{in}} \times 100(\%),$$

$$X_{H_2O} = \frac{c_{H_2O}^{in} - c_{H_2O}^{out} \bullet K}{c_{H_2O}^{in}} \times 100(\%)$$

where c_{EtOH}^{in} and $c_{H_2O}^{in}$ are the molar concentrations of ethanol and water in the reaction mixture (mol%); c_{EtOH}^{out} and $c_{H_2O}^{out}$ are the molar concentrations of ethanol and water in the post-reaction mixture (mol%); c_{CP}^{out} is the molar concentration of carbon-containing products in the post-reaction mixture (mol%); n is the number of carbon atoms in the carbon-containing molecule of the reaction product; K is the volume contraction factor ($K = c_C^{in}/c_C^{out}$, where c_C^{in} and c_C^{out} are the molar concentrations of carbon in ethanol fed to the reaction and in all carbon-containing compounds which were present in the post-reaction gases, respectively). The selectivity of ethanol conversion into individual carbon containing products was expressed as:

$$S_{CP} = \frac{X_{CP}}{X_{EtOH}} \times 100(\%)$$

The selectivity of hydrogen formation was determined as the ratio of the molar concentrations of hydrogen to the molar concentration of hydrogen containing reaction products:

$$S_{H_2} = \frac{c_{H_2}^{out}}{c_{H_2}^{out} + 2 \bullet c_{CH_4}^{out} + 2 \bullet c_{C_2H_4}^{out} + 2 \bullet c_{CH_3CHO}^{out} + 3 \bullet c_{C_2H_6}^{out} + 3 \bullet c_{C_2H_6}^{out} + 3 \bullet c_{C_3H_6}^{out} + 3 \bullet c_{CH_3COCH_3}^{out} + 4 \bullet c_{C_3H_8}^{out}} \times 100(\%)$$

3. Results and discussion

Nitrogen adsorption/desorption studies evidence typical mesoporous structure of the MCM-48 silica support and supported catalyst (Fig. 1). The isotherms display distinct step, which results from the capillary condensation in mesopores with narrow pore size distribution. The specific surface area of pure silica material (S_{BET} = 1283 m^2/g) decreases to 490 m^2/g after cobalt deposition. Similar changes are also observed for pore volume (the decrease from 0.93 cm^3/g to 0.33 cm^3/g). These phenomena reveal deposition of cobalt oxide species in the pores of the support. The presence of relatively large surface area after deposition may suggest that the channels of the silica materials are not completely filled with the oxide species of cobalt. There is still observed capillary condensation step on the isotherms [24]. The presence of the interconnected pores facilitates uniform deposition of precursors and formation of cobalt oxides in the silica support. The average pore diameter

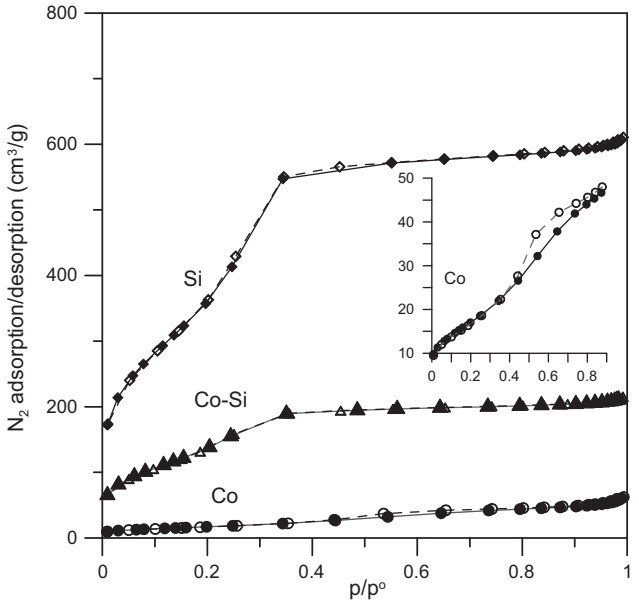

Fig. 1. Nitrogen adsorption/desorption isotherms for the silica support, Co–Si and Co catalysts (dashed curves and empty symbols – isotherms recorded with pressure decrease).

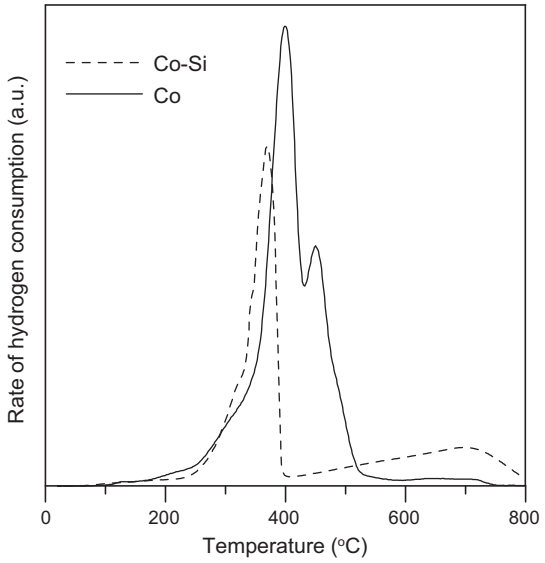

Fig. 3. Temperature-programmed reduction curves of the catalysts.

of both materials is similar (D_{BJHdes} = 2.4 nm and 2.5 nm, respectively).

The total surface area of materials after silica removal is at the level of 60.6 m^2/g. Pore volume is equal 0.09 cm^3/g. It is interesting that the isotherms still display the condensation loop, but located in the range of slightly higher partial pressures. The calculated average pore diameter is 4.6 nm.

The results of XRD studies show that phase composition of cobalt supported and unsupported systems are similar (Fig. 2). The position of the reflection lines correspond to the Co_3O_4 phase (#PDF 42-1467). Weak signal of (311) diffraction line and almost indistinguishable other lines, may indicate the presence of small, strongly dispersed species. The position of the reflection lines and peak width for the supported and unsupported systems are similar, suggesting that the size of the oxide species was not strongly changed after silica dissolution and thermal treatment. However, slight differences of the size, shape or chemical composition of the oxide species cannot be ruled out.

XPS analysis showed similar values of binding energies of cobalt in the supported and unsupported systems. The observed Co $2p^{3/2}$ peaks with binding energies of 780.0 eV for Co and 779.5 eV for Co–Si samples are characteristic for Co_3O_4 species. Relatively low surface Co/Si ratio (0.07) measured by the XPS indicates that cobalt oxide species are deposited in the channels of the silica support. This underlines the advantage of the application of the MCM48-type mesoporous silica matrices with interconnected uniform pores for the formation of 3D cobalt oxide nanostructures. The preparation of unsupported catalysts may resemble formation of skeletal catalysts, by leaching of Co–Al alloy with sodium hydrox-

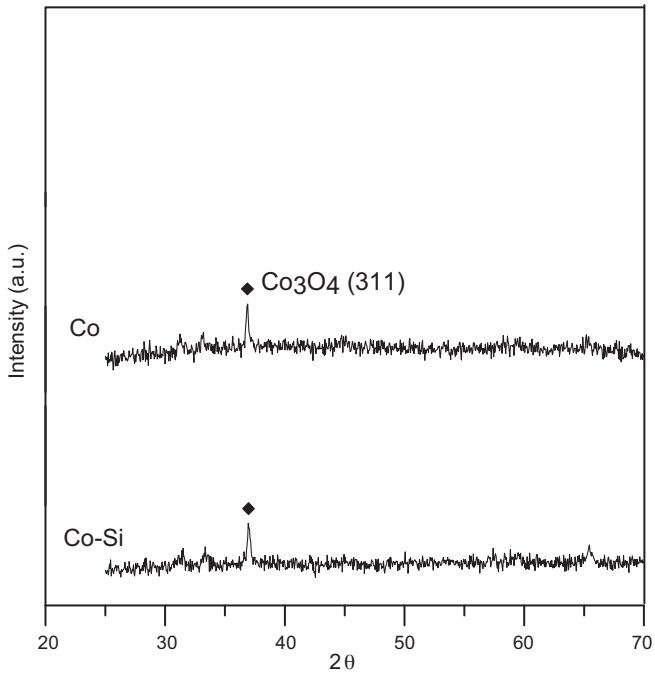

Fig. 2. XRD studies of the catalysts.

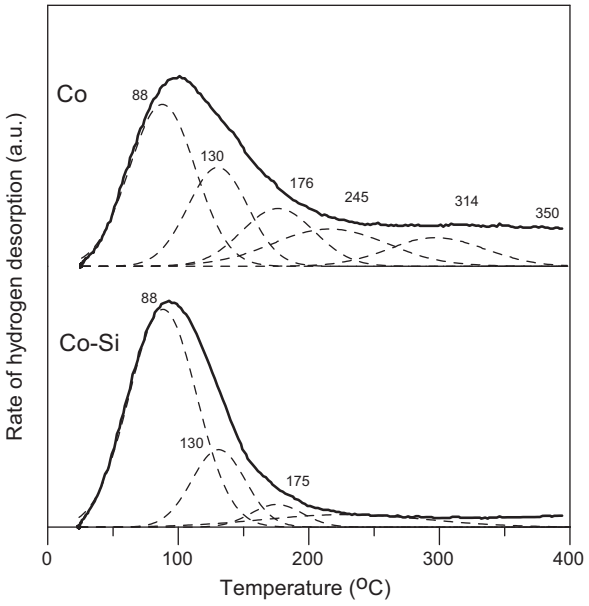

Fig. 4. Temperature-programmed desorption of hydrogen.

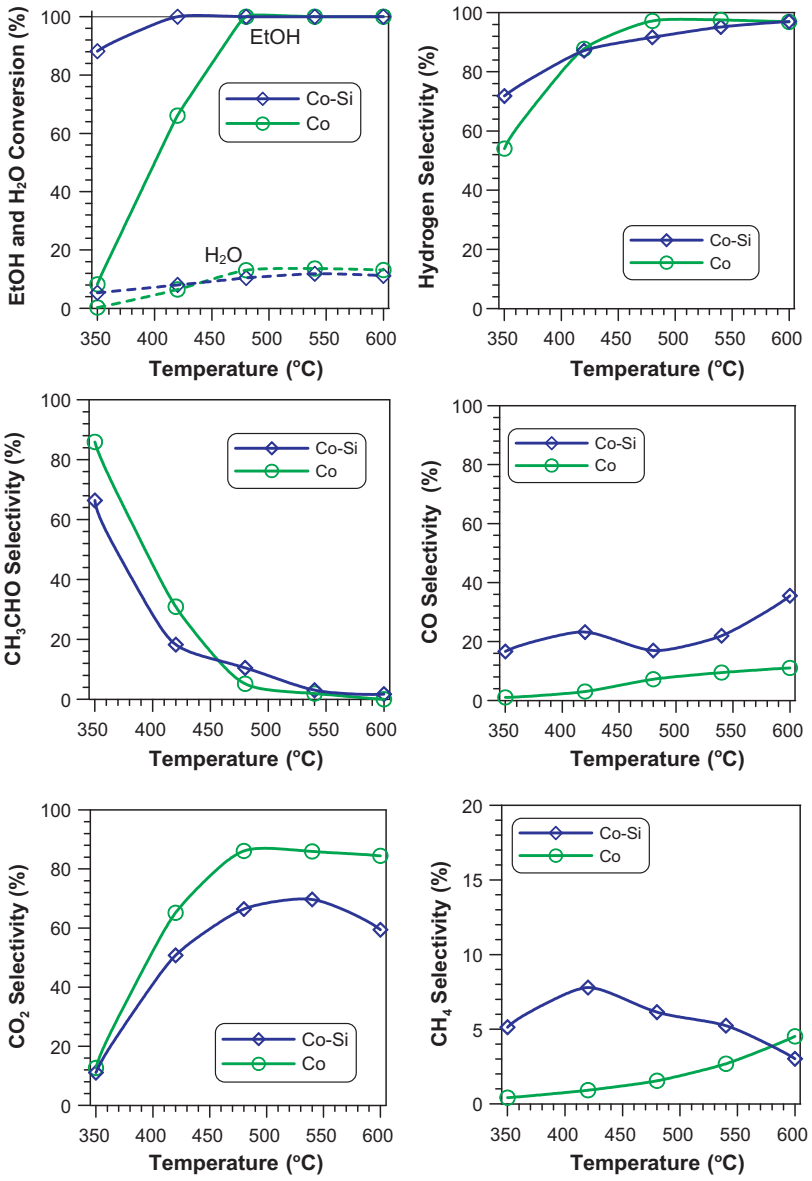

Fig. 5. Ethanol conversion and selectivity of supported (Co–Si), and unsupported catalysts (Co).

ide [25]. However, in our case the size and mutual arrangement of the oxide or metal species in the samples can be partially preserved after silica dissolution and much better controlled by application of matrices with suitable structural and chemical properties. The peaks of binding energies for Si 2s (153.0 eV) and Si 2p (102.1 eV) are not observed in the Co sample, after silica leaching. The obtained oxide samples contain the traces of Na, which might result from incomplete washing of NaOH.

Temperature programmed reduction studies confirm the presence of Co_3O_4 species in the Co–Si sample (Fig. 3). The irregular shape of the peak can be attributed to the reduction of Co_3O_4 to CoO and then to metallic cobalt. High temperature peak is connected with the reduction of strongly interacted CoO_x–SiO_2 species. The shape of the main reduction peak after silica removal (Co sample) is changed. The reduction of the Co sample starts at lower temperature, but the position of peak maximum moves from 370 °C to 399 °C, moreover the second reduction stage is more evident. Such behaviour is often attributed to the water diffusion effects in small pores [26]. The disappearance of high temperature maxima may indicate disruption of CoO_x–SiO_2 bonds and removal of the silica species.

The TPD of hydrogen studies are presented in the Fig. 4. The curves show the presence of a single nonuniform peak for the supported catalyst. The maximum of hydrogen desorption rate is located at around 100 °C. The desorption peak can be deconvoluted for three peaks, with maximum at 88 °C, 130 °C and 176 °C, respectively. The curves may indicate that cobalt crystallites located in the silica support, expose relatively weak and energetically uniform sites. The shape of hydrogen desorption peak in the unsupported systems is similar. However, it can be observed an increase of the number of strong adsorption sites.

The catalysts show relatively high activity in the ethanol steam reforming reaction (Figs. 5 and 6). Ethanol conversion in the presence of Co–Si catalyst approaches 90% at 350 °C, and 100% is observed at 420 °C. The reduced nanostructured cobalt oxides display lower initial activity; ethanol conversion at 350 °C is on the level of 10%. The main products at low temperature in both systems are hydrogen and acetaldehyde. The traces of acetic acid are

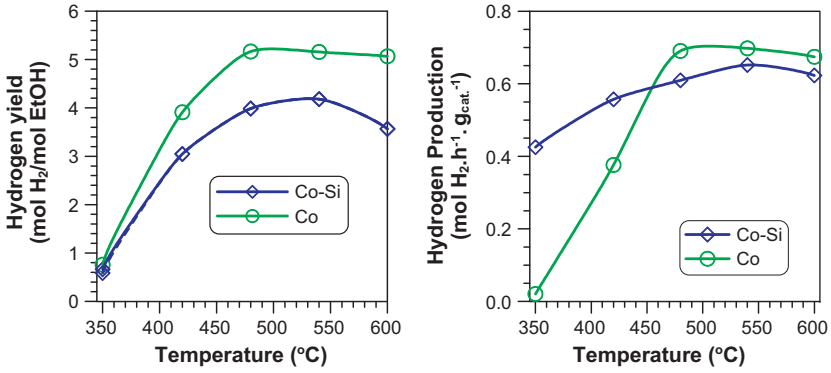

Fig. 6. Yield and production of hydrogen.

recorded at low temperature for the Co–Si catalyst. The selectivity of carbon containing products to CO in the presence of Co–Si catalyst increases from about 15 to 25% as the temperature increases from 350 to 420 °C, then slightly fall down, and next approaches 35% at 600 °C. The reaction at low temperature proceeds also toward methane, with 5% selectivity. The selectivity to methane after slight maximum at 420 °C decreases to a few percent at 600 °C. It is interesting that the production of higher hydrocarbons in the presence of both catalysts is below detection limit of GC. Ethylene is usually produced as by-product in the reaction of ethanol dehydration over acidic oxide surfaces. It also facilitates formation of carbon deposits. Both catalysts show similar selectivity to CO_2 at low temperature. The initial activity of the Co catalyst is lower, and high selectivity to CH_3CHO is observed. However, the Co sample shows better selectivity to CO_2 and lower selectivity to CO and CH_4 at elevated temperatures. The Co catalyst display lower selectivity to hydrogen at 350 °C. Better selectivity and higher hydrogen yield than for the Co–Si catalyst are observed above 420 °C.

The samples prior catalytic studies were reduced at 400 °C. Hence the catalysts in the reaction conditions could contain small fraction of difficult to reduce cobalt oxide species. The activation of ethanol and activation of water in the unsupported systems (Co samples) took place on the surface of cobalt species. The initial ethanol transformation to acetaldehyde in the dehydrogenation reaction occurred due to low-surface concentration of water (the conversion of water below 420 °C was very low). The unsupported oxides showed high selectivity to carbon dioxide and hydrogen at elevated temperatures. Such effect may result from the enhancement of the redox reactions, which occur on the surface of cobalt crystallites. The presence of water in the reaction condition may oxidise the surface of cobalt atoms [27]. Then surface carbon species (resulted from the transformation of ethoxide species) or carbon monoxide (produced in the decomposition reaction of ethanol or acetaldehyde $C_2H_5OH \rightarrow H_2 + CH_4 + CO$, $CH_3CHO \rightarrow CH_4 + CO$, reforming reaction of ethanol or acetaldehyde $C_2H_5OH + H_2O \rightarrow 4H_2 + 2CO$, $CH_3CHO + H_2O \rightarrow 3H_2 + 2CO$) can react with the surface oxygen, giving a new cobalt active site, ready for the adsorption of ethanol molecule or reaction with water molecule. Such effects are related to the cobalt–oxygen interactions. It has been often suggested that the reaction of steam reforming of ethanol in the supported systems takes place at the interface of the active metal and the support, which ensures oxygen from hydroxyl groups [28]. In the unsupported cobalt catalysts, the increase of oxygen mobility can be achieved by the suitable preparation methods or an introduction of promoters.

We have shown that the silica supported catalysts displayed better performance at low temperature. This effect could be attributed to the facilitation of activation and diffusion of water to the active cobalt sites. Taking into account such phenomena, an introduction of modifiers to the silica support, which can increase sorption and transport of water molecules to the periphery of cobalt crystallites, as well as an introduction of the species with oxygen storage properties (e.g. Ce or Ce–Zr oxides) may improve the performance of the catalysts.

4. Conclusions

The nanocasting technique was used for the preparation of cobalt oxide. The systems prior and after silica template removal were investigated. We have shown that cobalt catalysts, based on the supported mesoporous material with interconnected channels and that obtained after silica leaching showed relatively high selectivity to hydrogen and carbon dioxide. The activity of catalysts was related to the large surface area of silica support and the enhancement of the redox processes, which occur on the surface of small cobalt species.

References

[1] S. Sá, H. Silva, L. Brandão, J. Sousa, A. Mendes, Appl. Catal. B: Environ. 99 (2010) 43–57.
[2] M. Ni, D.Y.C. Leung, M.K.H. Leung, Int. J. Hydrogen Energy 32 (2007) 3238–3247.
[3] A.C. Basagiannis, P. Panagiotopoulou, X.E. Verykios, Top. Catal. 51 (2008) 2–12.
[4] P.D. Vaidya, A.E. Rodrigues, Chem. Eng. J. 117 (2006) 39–49.
[5] S.M. de Lima, A.M. da Silva, L.O.O. da Costa, J.M. Assaf, G. Jacobs, B.H. Davis, L.V. Mattos, F.B. Noronha, Appl. Catal. A: Gen. 377 (2010) 181–190.
[6] L. He, H. Berntsen, E. Ochoa-Fernández, J.C. Walmsley, E.A. Blekkan, D. Chen, Top. Catal. 52 (2009) 206–217.
[7] A. Denis, W. Grzegorczyk, W. Gac, A. Machocki, Catal. Today 137 (2008) 453–459.
[8] J.A. Torres, J. Llorca, A. Casanovas, M. Domínguez, J. Salvadó, D. Montané, J. Power Sources 169 (2007) 158–166.
[9] H. Wang, Y. Liu, L. Wang, Y.N. Qin, Chem. Eng. J. 145 (2008) 25–31.
[10] K. Urasaki, K. Tokunaga, Y. Sekine, M. Matsukata, E. Kikuchi, Catal. Commun. 9 (2008) 600–604.
[11] S.S.Y. Lin, D.H. Kim., S.Y. Ha, Catal. Lett. 122 (2008) 295–301.
[12] L.P.R. Profeti, E.A. Ticianelli, E.M. Assaf, Appl. Catal. A: Gen. 360 (2009) 17–25.
[13] A. Machocki, A. Denis, W. Grzegorczyk, W. Gac, Appl. Surf. Sci. 256 (2010) 5551–5558.
[14] M.N. Barroso, M.F. Gomez, L.A. Arrua, M.C. Abello, Chem. Eng. J. 158 (2010) 225–232.
[15] C.B. Wang, C.C. Lee, J.L. Bi, J.Y. Siang, J.Y. Liu, C.T. Yeh, Catal. Today 146 (2009) 76–81.
[16] S. Tuti, F. Pepe, Catal. Lett. 122 (2008) 196–203.
[17] M. Tiemann, Chem. Mater. 20 (2008) 961–971.
[18] P. Dibandjo, F. Chassagneux, L. Bois, C. Sigala, P. Miele, J. Mater. Chem. 15 (2005) 1917–1923.
[19] J.H. Smått, N. Schüwer, M. Järn, W. Lindner, M. Lindén, Micropor. Mesopor. Mater. 112 (2008) 308–318.
[20] I. Luisetto, F. Pepe, E. Bemporad, J. Nanopart. Res. 10 (2008) 59–67.
[21] J. Roggenbuck, H. Schäfer, T. Tsoncheva, C. Minchev, J. Hanss, M. Tiemann, Micropor. Mesopor. Mater. 101 (2006) 335–341.
[22] K. Schumacher, M. Grün, K.K. Unger, Micropor. Mesopor. Mater. 27 (1999) 201–206.

[23] S.J. Gregg, K.S.W. Sing, Adsorption, in: Surface Area and Porosity, Academic Press, London, 1982.
[24] H. Li, S. Wang, F. Ling, J. Li, J. Mol. Catal. A: Chem. 244 (2006) 33–40.
[25] A.J. Smith, L.O. Garciano, T. Tran, M.S. Wainwright, Ind. Eng. Chem. Res. 47 (2008) 1409–1415.
[26] L. Xue, C. Zhang, H. He, Y. Teraoka, Appl. Catal. B: Environ. 75 (2007) 167–174.
[27] D. Schanke, A.M. Hilmen, E. Bergene, K. Kinnari, E. Rytter, E. Ådnanes, A. Holmen, Energy Fuel 10 (1996) 867–872.
[28] H. Song, X. Bao, C.M. Hadad, U.S. Ozkan, Catal. Lett. (2010), doi:10.1007/s10562-010-0476-z).